Food Chemistry: X 19 (2023) 100770

Contents lists available at ScienceDirect

Food Chemistry: X

journal homepage: www.sciencedirect.com/journal/food-chemistry-x

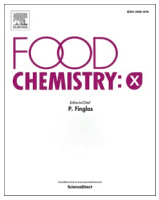

Spraying phenolic acid-modifiedchitooligosaccharide derivatives improves anthocyanin accumulation in grape

Songpo Duan, Zhiming Li, Zaid Khan, Chunmei Yang, Bosi Lu, Hong Shen *

College of Natural Resources and Environment, South China Agricultural University, Guangzhou 510642, China

ARTICLE INFO

Keywords:
Chitooligosaccharide derivatives
Phenolic acid
Antioxidant
Grapes
Anthocyanins

ABSTRACT

Herein, four chitooligosaccharide derivatives (COS-RA, COS-FA, COS-VA, COS-GA) were prepared by laccase-catalyzed chitooligosaccharide modification with rosmarinic acid (RA), ferulic acid (FA), gallic acid (GA), and vanillic acid (VA), and structures were characterized. RA and FA resulted in higher amino-substitution in the chitooligosaccharides than GA and VA. COS-RA and COS-FA had greater DPPH scavenging rates than COS-GA and COS-VA. Compared with COS treatment, spraying 250 mg L^{-1} COS-RA or COS-VA 6 times (once per 7 days) increased soluble sugar and anthocyanin content by 18.6%–23.2% and 41.7%–46.7%, respectively, from the fruit expansion to harvest stage. COS-RA and COS-VA also enhanced gene expression related to anthocyanin synthesis (*PAL, F3H, F3′5′H, DFR,* and *UFGT*) and monomeric anthocyanin accumulation (Mal-3-O-glu, Petu-3-O-ace-glu, Del-3-O-glu). Therefore, chitooligosaccharide derivatives may improve grape fruit anthocyanin accumulation by regulating antioxidant systems, improving the photosynthetic rate and inducing gene expression related to anthocyanin synthesis.

1. Introduction

Grape (*Vitis vinifera* L.) is one of the world's most economically important fruits, with approximately 7.4 million hectares planted worldwide and an annual production of approximately 77.8 million tons (Xia et al., 2021). China has the highest total grape production in the world and had a total grape production of 14.31 million tons in 2020 (from the website https://www.fao.org/faostat/zh/#data). In the southern part of China, excessive rainfall, long cloudy periods, low light intensity, low single-day temperature differences, and persistent high temperatures adversely affect the biosynthesis of primary and secondary metabolites that drive the production of sugar and the development of color in grapes, resulting in poor coloration, low sugar content, and delayed ripening (Deng et al., 2019; Teixeira, Eiras-Dias, Castellarin, & Gerós, 2013). The installation of rain shelters has reduced problems such as poor flower development and disease stress, but problems such as poor quality berries with insufficient color transfer still occur (Zhang et al., 2019). Therefore, new strategies to improve berry quality and color are urgently needed in southern China.

As a natural biostimulant, chitooligosaccharides (COS) are widely used in medicine, food, agriculture, and wastewater treatment due to their excellent water solubility, biocompatibility, and bioactivity (Yu et al., 2023; Zhang et al., 2020). In agriculture, chitooligosaccharides are considered eco-friendly plant growth regulators and stress inducers (Feng et al., 2019). COS has been reported to enhance photosynthesis, carbon metabolism, nitrogen metabolism, and the uptake of macro and micronutrient elements in plants (Ahmed, Khan, Siddiqui, & Jahan, 2020; Dzung, Khanh, & Dzung, 2011). This leads to the accumulation of soluble sugars and improved growth in crops such as wheat, coffee, and tea trees, etc. (Li et al., 2020; Zhang et al., 2016). Moreover, COS can also enhance abiotic stress tolerance in plants, including tolerance to drought stress, salt stress, cold stress, high temperatures, and heavy metal toxicity (Li et al., 2020; Zhang et al., 2016; Zou et al., 2015). Currently, there is a consensus that COS functions by elevating the activity of plant antioxidant enzymes (Zou, Tian, Dong, & Zhang, 2017), enhancing photosynthesis (Kim & Rajapakse, 2005) and stimulating the synthesis of secondary metabolites (Malerba & Cerana, 2016). This effect has been closely linked to the regulation of antioxidant activities by COS. Chitooligosaccharide functions of regulating antioxidant activity could be limited due to its low degree of polymerization, which can be modified by treating with different phenolic acids (Cui et al., 2022).

Rosmarinic acid (RA), ferulic acid (FA), gallic acid (GA), and vanillic acid (VA) are all widely recognized as natural phenolic acid antioxidants found in many different plants. The presence of carboxyl and hydroxyl

* Corresponding author.
E-mail address: hshen@scau.edu.cn (H. Shen).

https://doi.org/10.1016/j.fochx.2023.100770
Received 8 May 2023; Received in revised form 11 June 2023; Accepted 22 June 2023
Available online 25 June 2023

groups in these compounds provide them excellent antioxidant capacities. As a result, they are highly active and well-known substances in the field of plant antioxidants (Fachel et al., 2020; Vuolo,). However, the poor stability of these compounds, their weak biological permeability, and their low water solubility have led to low bioavailability and poor utilization efficiency (Amoah, Sandjo, Kratz, & Biavatti, 2016; Fachel et al., 2020). In this regard, based on the biocompatibility and water solubility of chitosan, we proposed to apply phenolic acid-based modifications to chitosan to enhance its antioxidant properties. Cases of physicochemically and biologically modified chitosan-polyphenol grafts have been reported in different studies (İlyasoğlu & Guo, 2019). By using techniques such as enzyme modification and free radical induction, polyphenols can be grafted onto a chitosan backbone (Hu & Luo, 2016). In a subsequent nonenzymatic reaction, laccase, a naturally occurring oxidoreductase of plant origin, can oxidize and rearrange phenols to form quinones and chitosan baramins to form chitosan-phenolic grafts by the Schiff base and Michael addition reactions (Božič, Gorgieva, & Kokol, 2012; İlyasoğlu & Guo, 2019).

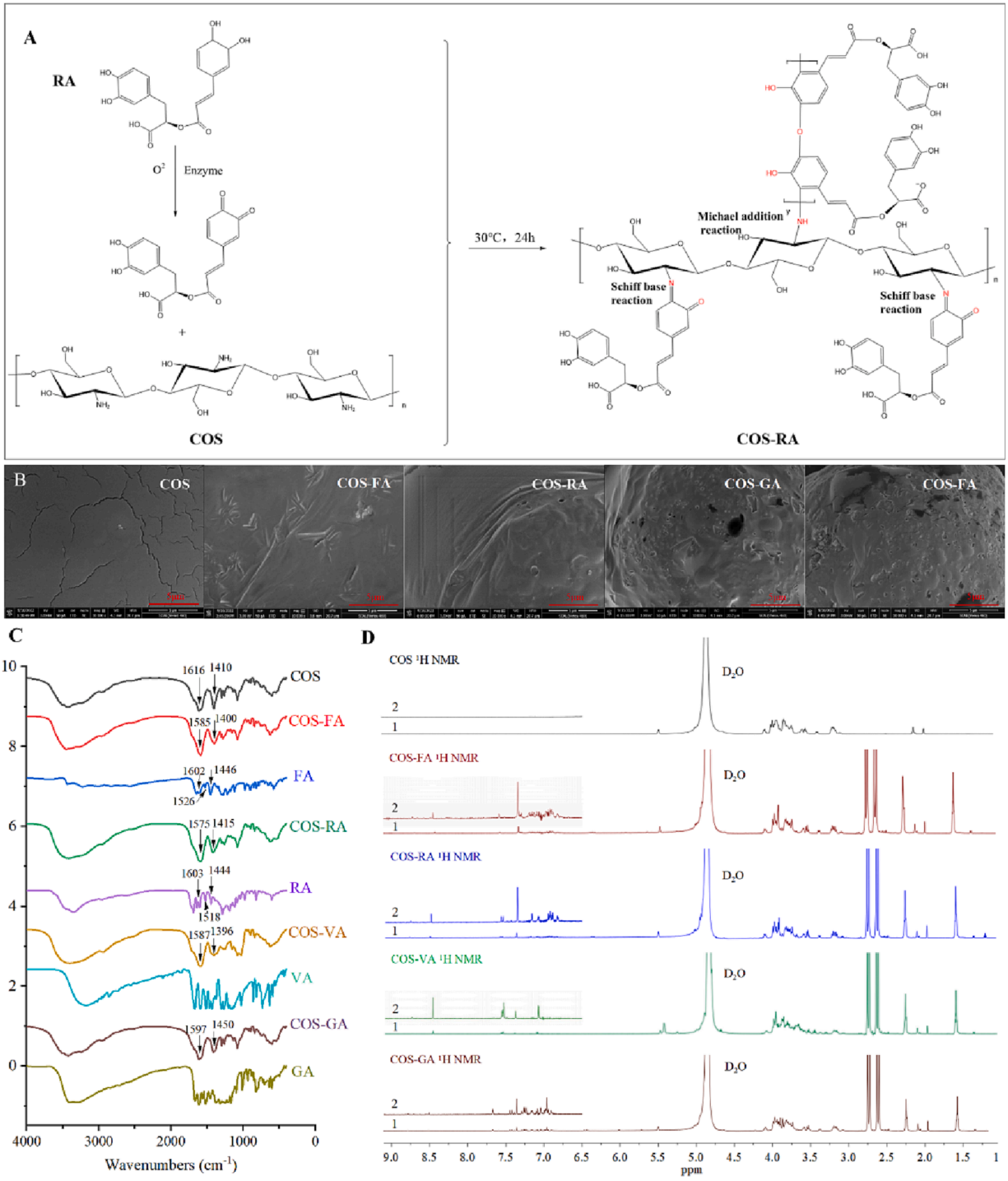

Fig. 1. Spectroscopic characterization and structure of chitooligosaccharide (COS), and chitooligosaccharide derivatives samples. (A) Synthesis diagram of COS-RA. (B) Scanning electron micrographs (SEM) of COS, COS-derivative samples (10,000×). (C) FT-IR spectra of COS, COS-derivatives, and phenolic acid samples. (D) ^{1}H NMR spectra of COS, COS-derivative samples, with 2 representing the amplified version of 1 in the COS-derivative spectrum.

Based on the idea of bioactive molecular grafting, various phenolic-modified chitosans have gained interest as superior antioxidant substances. Although several studies have demonstrated that phenolic-modified chitosan can prolong the postharvest freshness of fruits and decrease the occurrence of diseases during fruit storage, few studies have investigated the use of chitooligosaccharide modified with phenolic acids to improve fruit quality during growth and development. Therefore, this study aims to provide a new idea to explore the effect of spraying chitooligosaccharide derivatives on skin color, fruit quality and leaf growth and development of Kyoho grape, and to find a workable solution for insufficient coloring and poor quality of grapes in high temperature and rainy areas.

2. Materials and methods

2.1. Materials

Chitooligosaccharides (COS, Mw $\leq$ 2000 Da, degree of acetylation = 95%), vanillic acid (VA, purity $\geq$ 98%), gallic acid (GA, purity $\geq$ 99%), ferulic acid (FA, purity $\geq$ 99%), rosmarinic acid (RA, purity $\geq$ 97%), and 2,2-diphenyl-1-picrylhydrazyl (DPPH) (purity $\geq$ 96%) were purchased from Macklin Biochemical Co., Ltd, Shanghai (China). Laccase (120 U/g) was provided by Yuanye Biological Technology Co., Ltd., Shanghai (China). Dialysis bags (MWCO = 2000 Da) were obtained from Spectral Medicine, China. 'Kyoho' grapes were collected from Fengyi Ecological Park in Baiyun District, Guangzhou City, Guangdong Province.

2.2. Methods

2.2.1. Preparation of chitooligosaccharide - phenolic acid derivatives

COS derivatives were synthesized according to a previous method (Božič, Štrancar, & Kokol, 2013) with modifications. As a representative case, the preparation of chitooligosaccharide-rosmarinic acid derivatives (COS-RA) is described. The reaction was carried out at 30 °C for 24 h with 1 g (2000 Da) of COS dissolved in 100 mL of citrate buffer solution (0.1 mol L^{-1}, pH = 6.5). RA (1 mM) was steadily added, and laccase (9.6 U) was added while the solution was agitated continuously. The precipitate was removed from the solution by centrifugation at 5000 rpm for 5 min, condensed by a rotary evaporator, and dialyzed in deionized water (2000 Da) for 24 h to eliminate unreacted phenolic acids. The powder was then freeze-dried to produce COS-RA by the procedure shown in Fig. 1A. The same chemical technique was used to generate chitooligosaccharide-vanillic acid derivatives (COS-VA), chitooligosaccharide-gallic acid derivatives (COS-GA), and chitooligosaccharide-ferulic acid derivatives (COS-FA).

2.2.2. Scanning electron microscopy (SEM) analysis

SEM images of chitooligosaccharide derivatives were captured with a scanning electron microscope (Verios 460, FEI, Guangzhou, China). The samples were sputtered with a 20 nm thick gold layer and placed on an Al-Stub. The microscope was operated at accelerating voltages of 10 and 20 kV.

2.2.3. Elemental analysis

The carbon, hydrogen, and nitrogen mass ratios of COS and four COS derivatives were measured using an elemental analysis device (Vario EL III, Elementar Analysensysteme GmbH, Germany). The appropriate values were recorded, and the following equation was used to determine the degree of substitution (DS) of the samples:

$$DS = \frac{M_N R - (8 - 2DD)M_C}{n_C M_C}$$

DD is the degree of deacetylation of COS (95%); M_N and M_C are the molecular weights of nitrogen and carbon atoms, respectively. n_C is the atomicity of the carbon atoms of the phenolic acid; R is the ratio of C to N of the derivatives.

2.2.4. UV–vis spectroscopy

Before ultraviolet (UV)–visible spectroscopic investigation, vanillic acid (VA), gallic acid (GA), rosmarinic acid (RA), and caffeic acid (CA) were dissolved in ethanol (0.02 mg ml^{-1}) and COS (0.2 mg ml^{-1}) with COS derivatives (0.2 mg ml^{-1}) in aqueous solution. A Lambda 35 UV–vis spectrophotometer (PerkinElmer, Waltham, MA, USA) was then used to record the spectra in the 200–800 nm region with a beam width of 2 nm.

2.2.5. FTIR spectroscopy

FTIR spectroscopy was used to determine the functional groups in COS, phenolic acid, and COS derivatives. The IR spectra of the samples were obtained by a Vertex 70 instrument (Bruker, Germany). The selected wavenumber region was in the range of 4,000 to 400 cm^{-1} with 16 scans and a resolution of 4.0 cm^{-1}. All the tested samples were compacted with a certain percentage of potassium bromide.

2.2.6. ^1H NMR spectroscopy

^1H NMR was used to describe the structures of COS and the COS derivatives. The tests were conducted at 25 °C using an AVANCE NEO 600 MHz spectrometer (Bruker, Germany). D_2O was used as the solvent, and none of the solvent peaks interfered with the COS peaks.

2.2.7. Antioxidant activity determination

Different COS and COS-derivative solutions were prepared at different concentrations. An equal volume of 0.1 mmol L^{-1} DPPH methanol solution and 2 mL of COS-RA solution were vigorously mixed before being kept at room temperature and shielded from light for 30 min. The solution's optical density was then determined at 517 nm by UV-1600 spectrophotometer (UV-1600, Shimadzu, Japan). Methanol was used in place of the COS-RA solution to provide a control. The following calculation was used to compute the percentage of DPPH radicals that were scavenged:

$$\text{Scavenging effect } (\%) = \frac{A_{control} - A_{sample}}{A_{control}} \times 100$$

2.3. Plant materials and management

During the treatment period, field trials were carried out from mid-March 2022 to July 2022 in the vineyards of Fengyi Eco Park, Baiyun District, Guangzhou, Guangdong Province, China (23°28′24″ N, 113°25′28″ E), where there were more than 20 days of sunshine per month and the average daily maximum and minimum temperatures were 34 °C and 26 °C, respectively. Five-year-old 'Kyoho' grapevines were positioned at a distance of 3.5 m and 1.5 m apart under a rain shelter. At 50 days after flowering, five bunches of grapevines were chosen from each vine (close to the color-change stage). With one replicate for each plant and three replicates for a total of 12 plants, five clusters of grapes were chosen from each vine 50 days after flowering (close to the color-change stage). On May 22, from 6:30 to 7:30 p.m., the vines were exposed to water (control), 250 mg L^{-1} COS, COS-VA, and COS-RA solutions. The epidermis of the marked berries was sprayed with the treatment solution or water, and the leaves of the branches holding the treated grapes were sprayed on both sides. The first treatment (May 22) was considered day 0 after treatment, and leaf measurements and fruit sampling were performed 12 h later, with six sprays every seven days. On days 0, 15, 30, and 45 of treatment, 30 random samples of berries were taken from 20 labeled vines. The berry skins and pulp were separated, frozen in liquid nitrogen and kept at −80 °C.

2.3.1. Measurement of leaf-related indicators

Three functioning leaves from the side of the bunches were chosen before each spraying treatment to conduct measurements of photosynthetic indices. An LI-6800 portable photosynthesis measuring device (Li-6800, LI-COR, United States) was used to assess the net photosynthetic rate (P_n), stomatal conductance (G_s), and maximum quantum efficiency

(F_v/F_m) of photosystem II in grape leaves in five replicates. The SPAD 502 device was used to measure the amount of chlorophyll. Measurements were performed in clear weather between 10 am and 12 pm. The treated functional leaves were taken at maturity, and the leaf length, leaf width, and leaf area were measured using a portable leaf area meter (YMJ-B). Toluidine blue staining was used to examine the microstructure of leaves, and Slide Viewer software (3DHISTECH Ltd., Hungary) was used to calculate the thickness of leaves, fenestrations, and spongy tissue. The I2-KI colorimetric technique was used to calculate starch content (Whitaker et al., 2014). The leaves were homogenized in a 2 mL centrifuge tube with steel balls, heated in boiling water for 10 min, and centrifuged at 2,500 rpm for 2 min. Then, 50 μL of I2-KI was added to the supernatant to develop the starch, and the absorbance was measured at 594 nm. Leaf antioxidant enzyme activity was determined using the method of Liu et al. (2018). The crude enzyme solution was extracted as follows: 0.5 g of leaves was placed in 5 mL of 50 mmol/L phosphate buffer (pH 7.8, containing 1% polyvinylpyrrolidone (PVP)). The enzyme solution was extracted by following ice bath grinding, homogenized, and centrifuged at 12,000 × g and 4 °C for 20 min, and the supernatant was taken as the crude enzyme extract. Superoxide dismutase (SOD) activity was assayed by measuring its ability to inhibit the photochemical reduction of nitroblue tetrazolium, with 50% inhibition of the photochemical reduction of nitrotetrazolium blue chloride (NBT) defined as one unit of enzyme activity. One unit of enzyme activity for catalase (CAT) was defined as a decrease of 0.01 per minute in absorbance at 240 nm caused by a reduction in H_2O_2 extinction. The peroxidase (POD) activity was measured as an increase in absorbance at 470 nm due to guaiacol oxidation, defined as an increase in OD of 0.01 per minute as 1 unit of enzyme activity. Ascorbate peroxidase (APX) activity was measured by a decrease in absorbance at 290 nm upon ascorbic acid (ASA) oxidation, measured as the decrease in ASA per minute.

2.3.2. Determination of fruit quality parameters

Berry's weight was measured using an electronic scale. The soluble solids content (SSC) was measured using a digital refractometer (TD45, Guangzhou, China). The titratable acid (TA) content was determined by acid-base titration (Xia et al., 2020). The content of total soluble sugars was determined by the anthrone colorimetric method (Gao, 2006). The total anthocyanin content was evaluated using pH differential spectrophotometry (Xia et al., 2020). A reported method (Liu et al., 2019) was used to determine the levels of glucose, fructose, and sucrose. The supernatant was filtered after 1 g of pulp was homogenized with 5.0 mL of cold ethanol (80%) and incubated at 35 °C for 10 min. On an Agilent 1260 HPLC system with an NH2 column (4.6 mm × 250 mm, 5 μm, Agela Technologies, Shanghai, China), supernatants were analyzed. A mixture of acetonitrile and water (80:20, v/v) was used as the mobile phase, with a flow rate of 1 mL min^{-1}. The skin color of the berries was measured using a CM-2600d colorimeter (Konica Minolta, Tokyo, Japan). The a* values were recorded at two points along the equator and averaged.

2.3.3. Determination of anthocyanin composition

An amount of 0.3 g of berry sample was homogenized for 20 min with 3 mL of extraction solution (30:70:1, v/v/v) before being centrifuged and filtered. Anthocyanins were measured using a 250 × 4.6 mm Symmetry C18® column (Waters Corp., Milford, MA, USA) with a reported technique (Cho, Howard, Prior, & Clark, 2004). The mobile phase consisted of a binary gradient of 5% formic acid (A) and 100% methanol (B). The flow rate was 1 mL min^{-1}, and the linear gradient was from 2% B to 60% B over 60 min. The anthocyanin peak was quantified at 510 nm using a Waters Model 996 photodiode array detector (Milford). All anthocyanins were quantified as malvidin-3-glucoside equivalents using an external calibration curve for standards (Polyphenols-Laboratories AS, Sandnes, Norway) in the range of 5 to 125 μg mL^{-1}. Anthocyanin concentrations were expressed as mg malvidin-3-O-glucoside equivalents per gram of berry peel.

2.3.4. Gene expression analysis by qRT–PCR

In this study, the relative expression levels of 11 genes encoding anthocyanin synthesis (*PAL*, *CHS*, *CHI*, *F3H*, *F3′H*, *F3′5′H*, *DFR*, *LDOX*, *UFGT*, *MYBA1*, *MYBA2*) were determined. Total RNA was extracted using the plant-universal Bioteke Corp RNA kit (Takara, Guangzhou, China) and reverse transcribed using the Prime Script™ RT kit and the gDNA Eraser kit (Takara, Guangzhou, China). All primer sequences were obtained from NCBI (details are shown in Supplementary Table S3). Quantitative PCR was conducted using the SYBR premix ex Taq™ ii kit (Takara, Guangzhou, China). The amplification conditions were as follows: 95 °C for 30 s, followed by 40 cycles at 95 °C for 5 s and 60 °C for 30 s, followed by a final melting curve analysis. The $2^{-\Delta\Delta CT}$ method was used to calculate relative expression levels.

2.3.5. Statistical analysis

A completely randomized design was used to conduct the experiments. Each treatment was repeated three times; data are expressed as the means with standard deviations. Multiple comparisons were performed by one-way analysis of variance (ANOVA) and Duncan's multiple range test was applied at the 0.05 level of significance using SPSS version 19.0 (SPSS Inc., USA).

3. Results

3.1. Structural characterization and functions

The phenotypic characteristics of the COS and COS-derived samples are shown in Fig. 1B. The COS surface was relatively flat having more cracks under a scanning electron microscope at a magnification of 10,000. The surfaces of COS-RA and COS-FA were smooth with folds and no cracks following the oxidation of COS by laccase to graft phenolic acids (RA, GA, FA, VA). Additionally, the film was applied to the surface of COS-GA and COS-VA, but the surface was more fractured and uneven. The morphology of COS was modified differently by phenolic acids (RA, FA) with cinnamic acid as the parent nucleus relative to phenolic acids (GA, VA) with benzoic acid as the parent nucleus.

The elemental analysis results in Table S1 shows that the degree of substitution (DS) of phenolic acid-based COS-derivative products (COS-FA, COS-RA) with cinnamic acid as the parent nucleus was 0.282–0.287, which was a higher than that of chitosan grafted products (COS-VA, COS-GA) with benzoic acid as the parent nucleus (0.252–0.265), and the yield of the former was greater than that of the latter. This might be connected to the structure of the phenolic acids; they resemble cinnamic acid and are more readily converted to quinones by laccase and more readily grafted to COS.

The UV–vis absorption spectra of COS derivatives in comparison with those of phenolic acid and COS (Fig. S1A, B) suggested that novel chemical bonds were created by the COS derivatives. The n-π* transition of the C═O group gives rise to the characteristic absorption peak of COS at 281 nm (Zhao, Wang, Tan, Sun, & Dong, 2013). FA/RA shared three characteristic peaks at wavelengths of 219/220 nm, 237/242 nm, and 323/326 nm, which corresponded to the benzene ring system, the C═C double bond conjugated system, and the five conjugated systems of the phenolic acids with cinnamic acid as the parent nucleus, respectively (Saltas, Pappas, Daferera, Tarantilis, & Polissiou, 2013). In contrast to COS, the derivatives (COS-FA, COS-RA) displayed a redshift in the C═O group to the right at 284/285 nm, while the absorption peaks of FA and RA appeared at 320/323 nm (Fig. S1A). This shows that the grafts of FA and RA onto COS were successful. The two characteristic peaks displayed by VA and GA, which represent benzoic acid as the parent nucleus of the benzene ring system and four conjugated systems, respectively, were found near 231/218 nm and 277/272 nm. New peaks were produced at 308 nm and 311 nm when VA and GA were grafted onto the chitooligosaccharide. COS-VA and COS-GA underwent a redshift to 285/283 nm (Fig. S1B). Due to the coupling of C—C with C—O—C, the two shifts were associated with the n-π* transition,

indicating that the side chain of phenolic acid reacted and that VA was successfully grafted to COS with GA.

The FTIR absorption spectra of COS, COS derivatives, and phenolic acids are displayed in Fig. 1C. The COS spectra exhibited absorption peaks at 1616 and 1410 cm^{-1}, which are attributed to the residual *N*-acetyl group's C═O stretching mode (amide I band) and the N—H deformation mode (amide II band), respectively (Liu, Lu, Kan, Tang, & Jin, 2013). The presence of aromatic rings in the molecule causes the three absorption bands at 1603/1602, 1518/1526, and 1444/1446 cm^{-1} in RA and FA, indicating the presence of aromatic ring stretching in the molecule (Wang, Mao, Dai, Yuan, & Gao, 2018). Compared to pure COS, COS-RA and COS-FA have slightly different spectra. The characteristic peaks at 1616 cm^{-1} were slightly shifted to the right at 1575 and 1585 cm^{-1}; this was attributed to the rightward shift caused by the overlap of RA with the benzene ring in FA and the characteristic peak of C═O in COS. The N—H (1410 cm^{-1}) deformation of COS-RA and COS-FA caused a decrease in the characteristic absorption band, suggesting that the amino group was largely replaced by RA and FA. These findings imply that a Schiff base or Michael-type reaction takes place when the COS amino group reacts. The characteristic peak at 1616 cm^{-1} shifted to the right to 1587 and 1597 cm^{-1} in COS-VA and COS-GA, and the N—H deformation at 1396 and 1405 cm^{-1} resulted in a narrower characteristic absorption band. These results indicate that COS was successfully grafted and modified with phenolic acids.

The ^1H NMR spectra of COS and its derivatives were obtained, and Fig. 1D depicts the distinctive peaks of the COS functional groups. The multiple peaks from 3.32 to 4.05 ppm represent the protons from H3 to H6 in the hypo methyl groups of glucosamine (GlcN) and in *N*-acetylated glucosamine (*N*-acetylated GlcN), and the peak at 4.79 ppm represents the solvent D_2O. The methyl protons on the *N*-alkylated glucosamine residues, the protons in GlcN's H2 and H1, and those in *N*-acetylated GlcN are represented by single peaks at 2.05, 3.10, and 4.59 ppm (Liu, Xia, Jiang, Yu, & Yue, 2018). When grafted rosemary acid was subjected to laccase oxidation, multiple proton characteristic peak signals at 6.77–7.50 ppm were found in the COS-RA region 2, which belonged to the aromatic protons of conjugated RA. These signals were shifted to the right and were in a lower region in comparison to the RA spectrum (5.5–6.4 ppm), and the new chemical shifts imply that the RA protons were still bound to COS. Additionally, COS-FA (6.79–7.50), COS-VA (6.90–7.50), and COS-GA (6.78–7.50) all had similar proton characteristic peaks, proving that these phenolic acids were successfully grafted onto COS (Fig. 1D). In conclusion, the detailed SEM, elemental analysis, UV–visible spectroscopy, FI-TR, and ^1H NMR characterization results demonstrated that both phenolic acids (RA, FA) with cinnamic acid as the parent nucleus and phenolic acids (GA, VA) with benzoic acid as the parent nucleus were successfully grafted onto the COS skeleton, with RA and FA exhibiting a higher degree of grafting than GA and VA.

A DPPH radical scavenging assay was performed following the successful grafting of chitosan phenolic acid to examine the molecule's antioxidant capacity (Fig. S2). COS and its derivatives' DPPH scavenging capacity depends on concentration and rises with concentration. Within 30 min, the DPPH consumption of the COS-RA solution at 0.25 mg ml^{-1} reached 69.8%, which was approximately 13.0, 3.5, 2.6, and 1.9 times greater than that of COS, COS-VA, COS-GA, and COS-FA, respectively. Therefore, phenolic acid modification enhanced the antioxidant capacity of COS, showing the same trend as the amino substitution of COS derivatives (COS-RA > COS-FA > COS-GA > COS-VA > COS).

3.2. Antioxidant system and physiological and biochemical characteristics of grape leaves

The antioxidant enzyme activities and the accumulation of H_2O_2 and O_2^- in leaves were evaluated to investigate the effects of COS and its derivatives on the antioxidant system of functional grapevine leaves. Spraying COS and its derivatives improved the activities of antioxidant enzymes (SOD, CAT, and POD; APX activity had no discernible impact) and decreased the concentrations of H_2O_2 and O_2^- in the leaves, as shown in Table 1. After 12 h of COS-VA and COS-RA treatments, leaf SOD, POD, and CAT enzyme activities increased in comparison to COS by 8.8%–10.4%, 18.3%–23.1%, and 23.2%–31.6%, respectively; in contrast, H_2O_2 and O_2^- content dropped collectively by 37.6%–43.1% and 36.2%–42.8%. This finding suggests that spraying COS-VA with COS-RA can substantially boost antioxidant enzyme activity in leaves, lessen H_2O_2 and O_2^- stress in leaves, and improve the growth performance of grape under stress conditions.

The morphology of the functional leaves at maturity was examined, and the spraying of COS and its derivatives had an impact on the morphological development of grape leaves. (Fig. S3A). The thickness of leaf fenestrated, and spongy tissue was found to be increased by COS, COS-VA, and COS-RA treatments. Both treatments were more effective than COS, thickening the corresponding tissues by 13.8%–20.7%, 9.3%–12.9%, and 21.8%–34.1%, respectively (Fig. S3B–D). Grape single leaf weight (11.8%–17.9%) and leaf area (14.0%–15.7%) increased more in the COS-VA and COS-RA treatments than in the COS treatment, although the differences between COS and the control were not statistically significant (Fig. S3E–F).

The phenological stage and treatment had a significant impact on the net assimilation rate (P_n), stomatal conductance (G_s), the maximum quantum yield of PSII (F_v/F_m), and chlorophyll content (SPAD) (Fig. S4). The trends in P_n, G_s, and F_v/F_m were consistent as influenced by the phenological stage, increasing first up to 15 days and then slowly decreasing, while the SPAD values increased first and then stabilized. After 15 days of COS-VA and COS-RA treatment, P_n, F_v/F_m, and SPAD were affected by the treatments and began to increase significantly relative to those in the COS treatment ($p < 0.05$). The increasing trend persisted over time. When compared to the COS treatment, the P_n, F_v/F_m, and SPAD of COS-VA and COS-RA at maturity (45 days) increased by 25.1%–29.2%, 4.3%–4.5%, and 6.7%–8.5%, respectively. Moreover, compared to the COS treatment, the COS-VA and COS-RA treatments increased the levels of leaf sucrose (20.8%–28.1%), soluble sugar (24.5%–26.3%), and starch (11.2%–14.4%) (Table S2).

According to the aforementioned findings, COS-RA and COS-VA improve the leaf antioxidant system, promoting the development of fenestrated and spongy tissues, which in turn raises the chlorophyll content and photosynthetic intensity of leaves, allowing the leaves to accumulate more assimilable products that can transport to the fruits.

3.3. Fruit quality

After 15 days of COS-VA and COS-RA treatment, the SSC content increased significantly in comparison to COS ($p < 0.05$), while TA decreased after 30 days of treatment (Fig. 2A, B). This increase in the SSC to TA ratio improved grape flavor. In line with SCC, COS-VA and COS-RA increased the amount of soluble sugar, particularly sucrose, in the berry pulp as the fruit ripened. At 45 days, sucrose content increased by 97.1%–102.9% compared to COS treatment, while fructose and glucose content rose by 19.7%–22.0% and 15.1%–21.1%, respectively (Fig. 2D–G). It is interesting to note that, compared to COS treatment, the total anthocyanin content of grapes increased rapidly after 15 days of COS-VA and COS-RA treatments, with a significant increase of 41.7%–46.7% at 45 days ($p < 0.05$). Additionally, there was no discernible difference in the weight of a single grape berry between treatments (Fig. 2D). According to these findings, COS, COS-VA, and COS-RA treatments all enhanced the amount of soluble sugar and total anthocyanin in grape berries, both treatments were more effective at the same concentration.

3.4. Berry peel color and anthocyanin content

According to Fig. 3A, after 15 days of COS-VA and COS-RA treatment, the berries' epidermal section quickly turned light red in

Table 1
Antioxidant system for leaf blades.

Treatments	SOD activity (U·mg^{-1} min^{-1})	POD activity (U·g^{-1} min^{-1})	CAT activity (U·g^{-1} min^{-1})	APX activity (U·g^{-1} min^{-1})	H_2O_2 content(μmol·g^{-1} FW)	O_2^- content (μmol·g^{-1} FW)
Control	562.80 ± 9.36c	442.43 ± 6.63c	5.46 ± 0.14b	0.78 ± 0.02a	92.06 ± 3.04a	84.36 ± 3.97a
COS	633.10 ± 8.72b	498.40 ± 8.84b	5.99 ± 0.21b	0.74 ± 0.02a	81.13 ± 1.72b	71.43 ± 1.88b
COS-VA	685.93 ± 4.74a	587.33 ± 5.24a	9.69 ± 0.21a	0.82 ± 0.04a	54.73 ± 2.32c	47.10 ± 2.62c
COS-RA	698.76 ± 4.60a	614.87 ± 5.76a	10.66 ± 0.33a	0.80 ± 0.03a	47.70 ± 2.63c	40.73 ± 2.37c

Letters behind the values in the same column indicate significant differences among different treatments, $p < 0.05$.

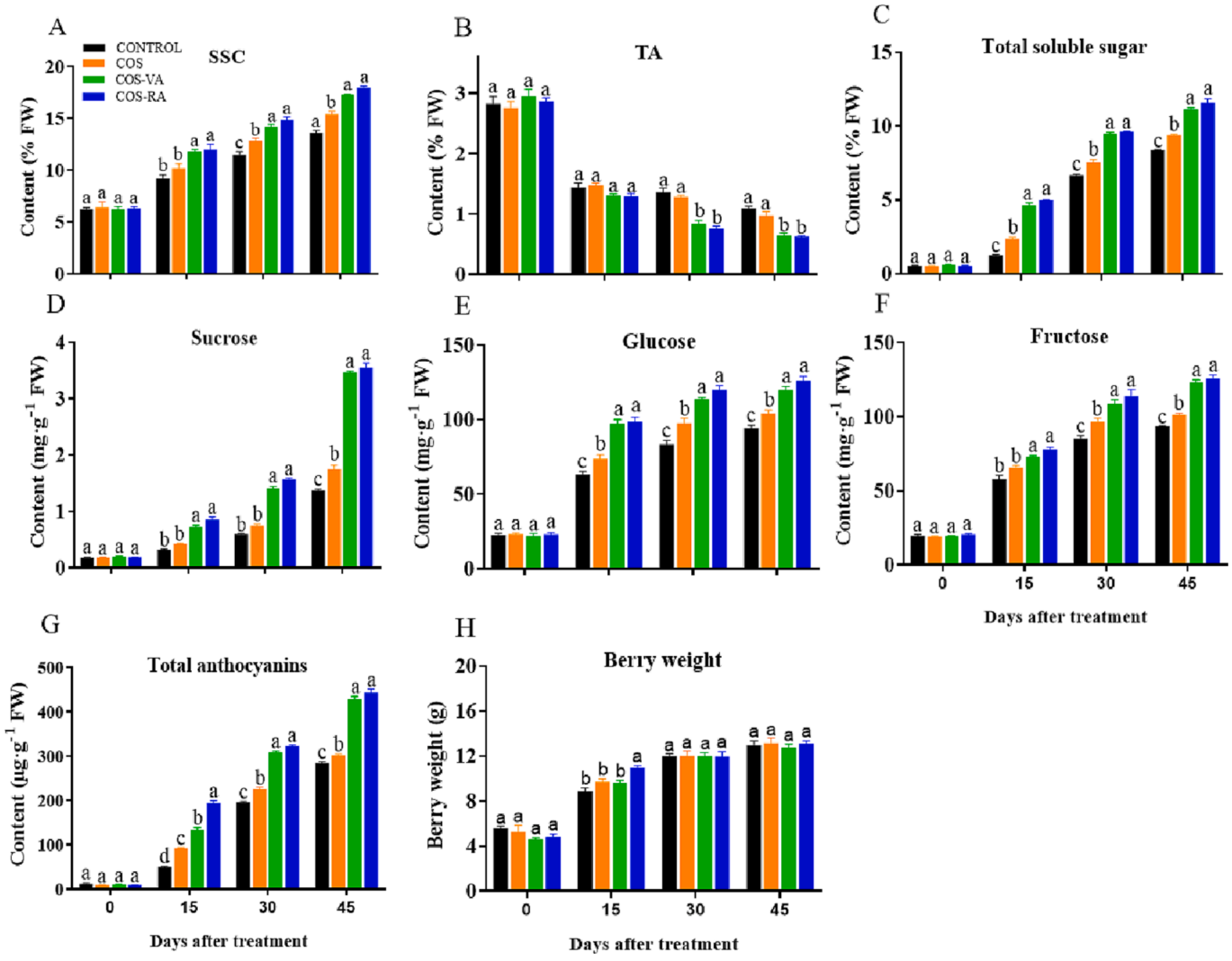

Fig. 2. Effect of COS, COS-VA, and COS-RA on fruit quality indexes. (A-H) soluble solids (SSC), titratable acid (TA), soluble sugars, sucrose, fructose, glucose, total anthocyanin content, and single fruit weight. Different lowercase letters indicate significant differences among the treatments, based on the Duncan test ($p < 0.05$, n = 4).

comparison to the control and COS treatment; at 45 days, the berries treated with COS-VA and COS-RA were darker than those of the control and COS treatment. Therefore, COS-VA and COS-RA spraying considerably raised the a* values from 15 to 45 days (Fig. 3B), and the values increased by 17.2%–18.3% at 45 days compared to COS treatment. After 15 days, the COS, COS-VA, and COS-RA treatments significantly increased the total anthocyanin content (Fig. 2G) in the skin of mature grapes ($p < 0.05$), and the contents of five monomeric anthocyanosides were increased to varying degrees. The predominant anthocyanin components found were Petu-3-O-ace-glu, Del-3-O-glu, and Mal-3-O-glu, which responded more strongly to COS-VA and COS-RA treatments, with 74.1%–84.2%, 46.3%–58.0%, and 39.5%–47.3% increases, respectively, at 45 days compared to COS (Fig. 3C–E). Peo-3-O-glu and Cya-3-O-glu, on the other hand, were relatively less influenced by COS-VA and COS-RA treatment, increasing by 7.9%–13.5% and 9.3%–14.4%, respectively, compared to COS (Fig. 3F, G). This demonstrates that COS-VA and COS-RA increase anthocyanin accumulation in grape skins by increasing the levels of Petu-3-O-ace-glu, Del-3-O-glu, and Mal-3-O-glu.

3.5. *Expression levels of anthocyanin-related genes*

The expression levels of nine anthocyanin synthesis-related genes (*PAL*, *CHS*, *CHI*, *F3H*, *F3′H*, *F3′5′H*, *DFR*, *LDOX*, *UFGT*) and two regulatory genes (*MYBA1*, *MYBA2*) were determined by qRT–PCR (Fig. 4). The

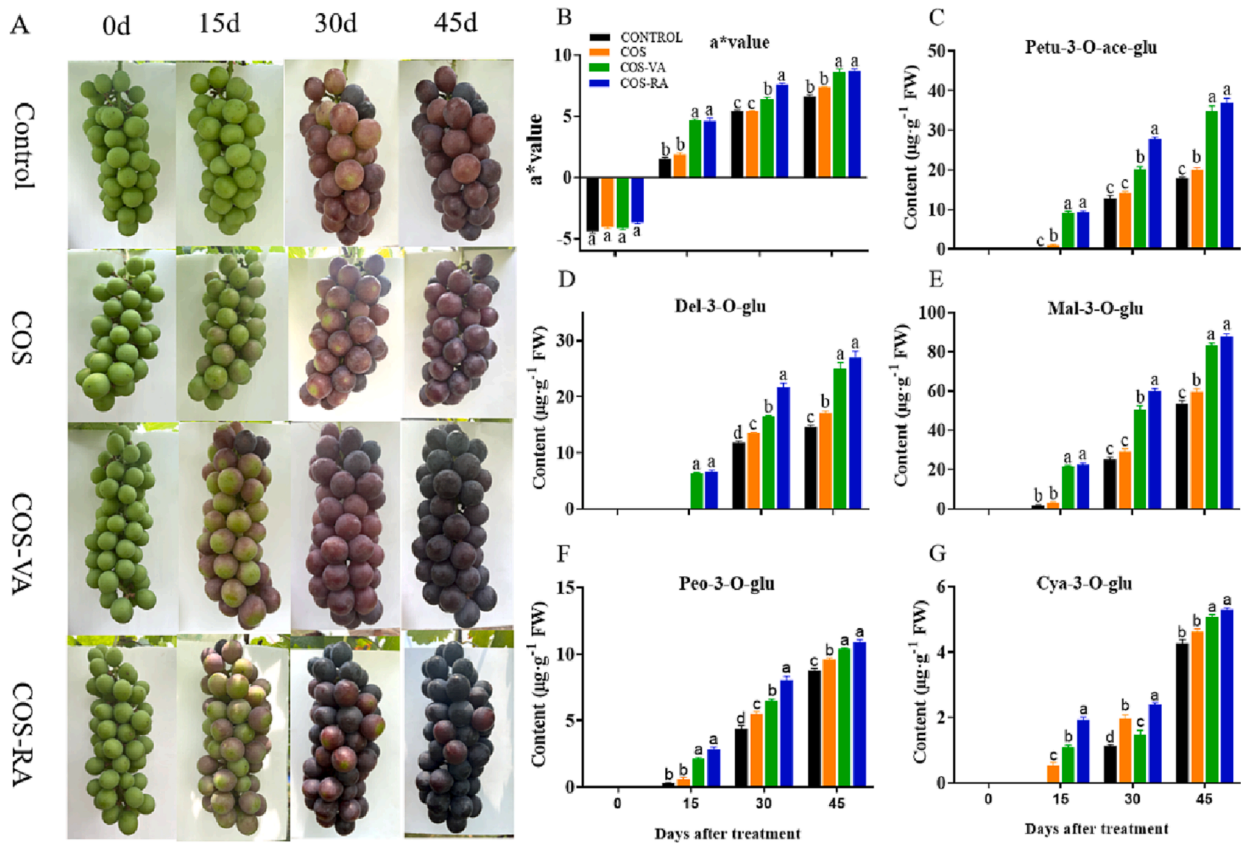

Fig. 3. Effect of COS, COS-VA, and COS-RA on grape color (A), a* value (B), and monomeric anthocyanin content (C-G). Different lowercase letters indicate significant differences among the treatments, based on the Duncan test ($p < 0.05$, n = 4).

initial stage of anthocyanin production involves the phenylalanine conversion route, and VvPAL was considerably enhanced by COS-VA and COS-RA treatments throughout the period compared to COS treatment, and the difference was most significant at 15 days, approximately 6.26–6.60 times that of COS (Fig. 4A). In the second stage, in the basic upstream flavonoid pathway, the transcript abundance of dihydromyricetin and dihydrokaempferol synthesis-related genes (*CHS*, *CHI*, *F3H*, *F3′5′H*) was significantly higher after 15th days of COS-VA and COS-RA treatment than after the control and COS treatment (Fig. 4B–F). Especially at 15th day of treatment, VvF3H and VvF3′5′H expression was approximately 2.13–2.51 and 2.81–3.26 times higher than that of COS treatment. Nevertheless, the expression level of the dihydroquercetin regulatory gene VvF3′H was not affected, which resulted in a lower accumulation of Peo-3-O-glu and Cya-3-O-glu. As a result of the COS-VA and COS-RA treatments, VvUFGT expression levels were consistently greater than those of COS treatment at 30–45 days and approximately 3.98–4.39 times higher than those of COS treatment at 45 days. Two regulatory factors, VvMYBA1 and VvMYBA2, demonstrated a considerable increase from 15 to 30 days and a decrease at 45 days. These results suggest that COS-VA and COS-RA treatments influenced gene expression throughout the grape peel anthocyanin production stage, favoring high expression of the *PAL*, *F3H*, *F3′5′H*, and *UFGT* genes in particular.

3.6. Principal components analysis

The effects of COS, COS-VA, and COS-RA spraying on antioxidant, photosynthesis, fruit sugar, and anthocyanin gene expression in grapevine leaves were evaluated using PCA. Fig. 5 displays the distribution of the examined physicochemical parameters and component load for the two components (PC). The top two PCs (PC1 = 79.5% and PC2 = 7.6%) explained 87.1% of the variation in the data. PC2 accounted for a small proportion of the variance (7.6%), but PC1 explained the variance in the majority of the qualities under investigation. PC1 explained a reasonably high proportion of the variance (79.5%). According to the various treatment distributions, COS-VA and COS-RA scored positively in PCA1, but COS and the control scored negatively. This indicates that COS-VA and COS-RA significantly improved grape index features, although there was no statistically significant difference between the two treatments. As shown in Fig. 5B, loading analysis revealed an acute angle between total anthocyanin content and leaf antioxidant enzymes (SOD, POD, CAT), photosynthesis (P_n, F_v/F_m, SPAD), fruit sugars (sucrose, fructose, glucose), and anthocyanin synthesis genes (*PAL*, *CHS*, *CHI*, *F3H*, *F3′5′H*, *DFR*, *LDOX*, *UFGT*, *MYBA2*). In other words, the anthocyanin gene expression, fruit sugar content, photosynthesis, and antioxidant system of the leaf all positively influenced overall anthocyanin accumulation. The angle between the leaf antioxidant system and photosynthesis, fruit sugar, total anthocyanin, anthocyanin synthesis gene, and total anthocyanin content was small and extremely positively correlated.

4. Discussion

During the summer season in southern China, changes occur in the microclimate of vineyards and increase the potential for high-temperature and low-light conditions to occur, which affects the basic physiological functions of the vine and the accumulation of substances such as glucose and anthocyanins, causing issues such as lower color development and poor quality of grapes at ripening (Deng, et al., 2019; Palliotti, Tombesi, Silvestroni, Lanari, Gatti, & Poni, 2014). Many studies have demonstrated that the application of exogenous compounds, such as phytohormones, biostimulants, derivatives, and synthetic agents, can boost plant life activities, lessen stress damage, and improve fruit quality (Ahmed, Khan, Siddiqui, & Jahan, 2020; Cui et al.,

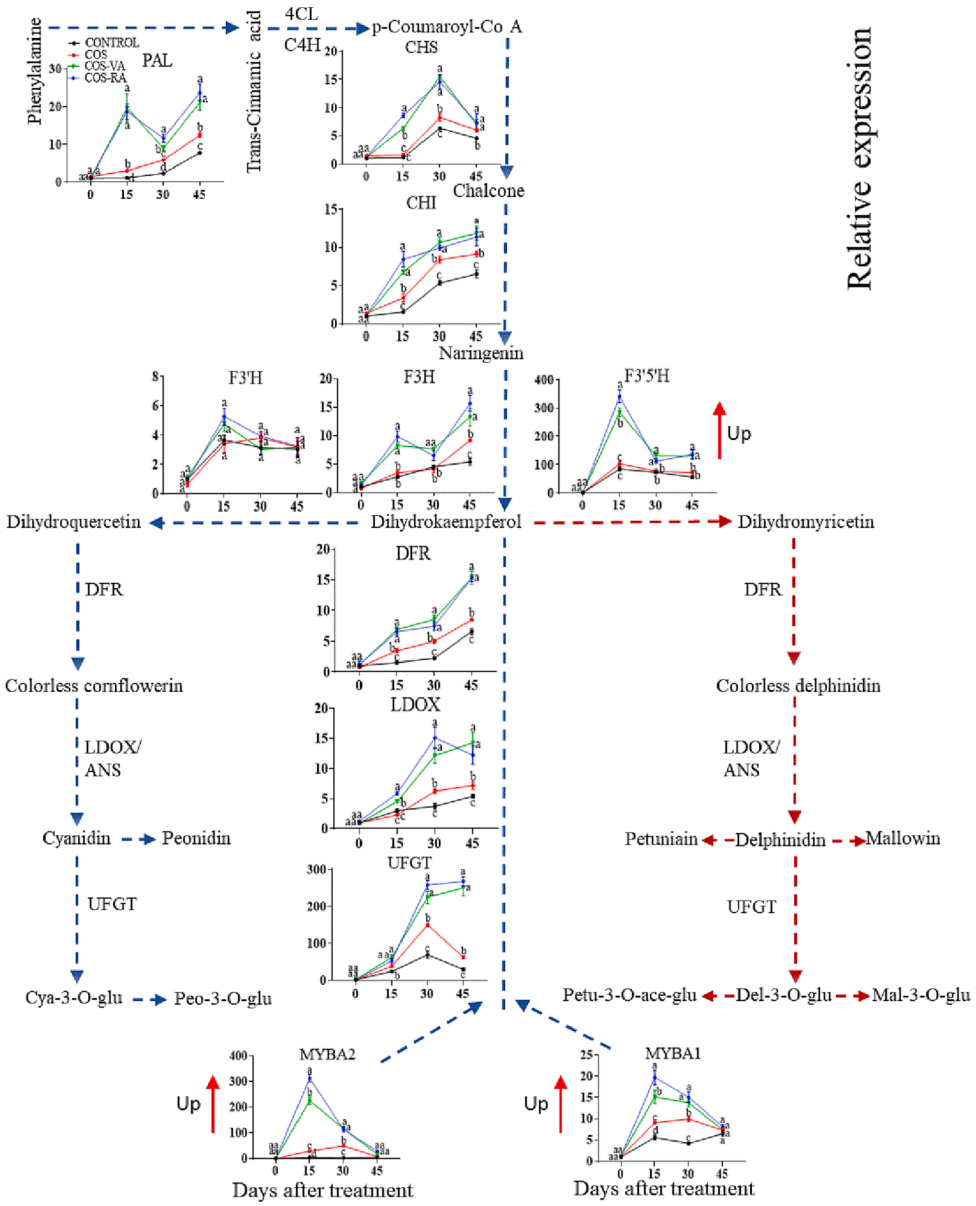

Fig. 4. Transcript levels of anthocyanin-related genes in berry skin. X-axis and Y-axis represent the days after treatment and the expression fold change relative to Control (0 Day), respectively. Different lowercase letters indicate significant differences among the treatments, based on the Duncan test ($p < 0.05$, n = 4).

2022).

In this research work, a novel class of chemicals was synthesized, which included COS-RA, COS-FA, COS-VA, and COS-GA. COS was modified with phenolic acid (Fig. 1A) and oxidized with laccase to form quinones from phenolic acid, and chitosan-phenolic derivatives were formed through Schiff base and Michael addition reactions. Due to differences in the apparent morphology (Fig. 1B), substitution level (Table S1), and valence bond changes (Fig. 1C, D and Fig. S1) among COS-RA, COS-FA and COS-VA, COS-GA and differences in structure and substitution, the former had approximately doubled antioxidant activity of the latter, and the activities of both were higher than that of COS (Fig. S2). The phenolic acids (RA, FA) with cinnamic acid as the parent nucleus were more easily oxidized by laccase than those with benzoic acid as the parent nucleus (GA, VA), and the former was more grafted to COS. Their antioxidant capacity showed the same trend as that of amino-substituted COS derivatives which might have caused these significant differences. Most researchers agree that phenolic acid's strong antioxidant activity is determined by its structure, and the structure of most chitosan derivatives is similar to that of chitosan (Huerta-Madronal, Caro-Leon, Espinosa-Cano, Aguilar, & Vázquez-Lasa, 2021).

Grape leaves and fruits were sprayed with 250 mg L^{-1} COS-RA, COS-VA, and COS solution 50 days after flowering to investigate the impact of these two novel compounds on grape development and quality. Chitosan and chitooligosaccharides are inducers of plant defense responses, and most studies have shown that chitosan treatment can trigger rapid production of hydrogen peroxide in plant leaves, which acts as a signaling molecule to trigger the ROS scavenging system, causing upregulation of superoxide dismutase (SOD), peroxidase (POX) and catalase (CAT) activities and resulting in a sustained period of high free radical scavenging activity in plants (Frederickson Matika, & Loake, 2014). In this study, we discovered that treatments with COS-RA, COS-VA, and COS increased the antioxidant enzyme (SOD, POD, and CAT) activities of leaves (Table 1). The enzyme activities of treatments with COS-RA and COS-VA were higher than those of treatments with COS, which may be related to the potent antioxidant properties of the chitosan phenolic acid derivatives. Enhanced antioxidant capacity in leaves can prevent oxidative damage caused by a variety of stimuli and preserve the leaves' ability to photosynthesize. Under varying climatic

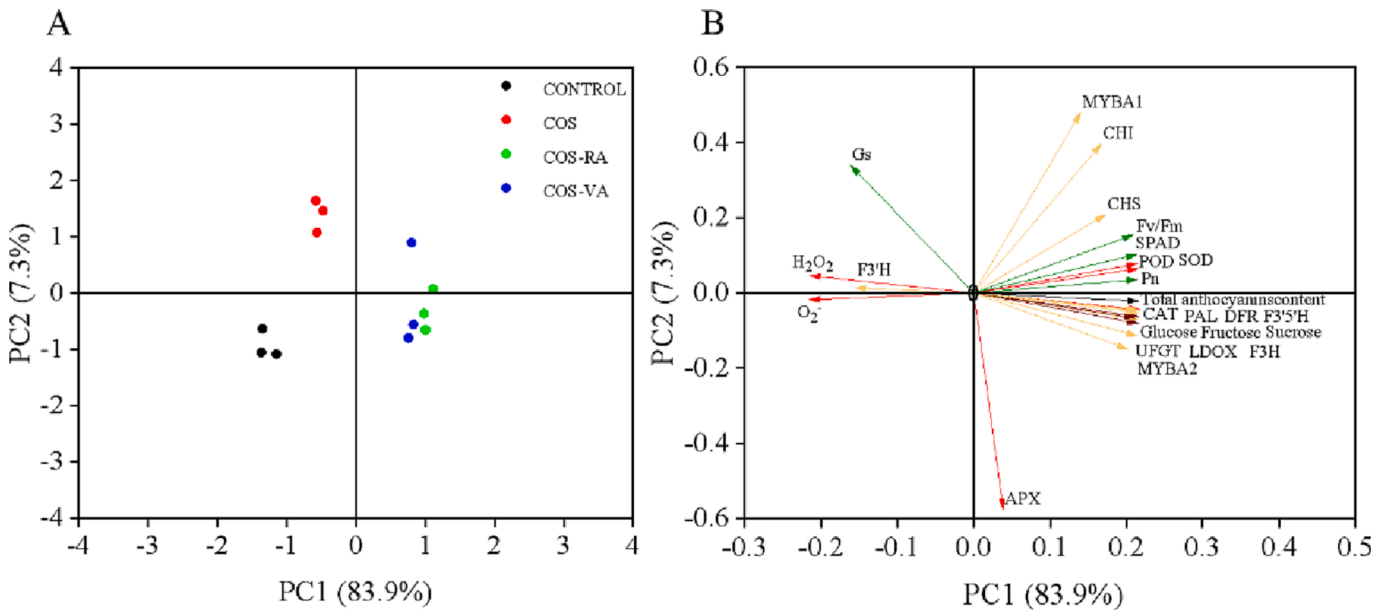

Fig. 5. Plots of principal component analysis of leaf antioxidant system, photosynthesis, fruit sugar, genes related to anthocyanin synthesis, and total anthocyanin-related indicators. Distribution of principal component analysis scores of relevant indicators with different treatments (A), principal component loading plot (B).

conditions, maintaining high antioxidant capacity may guarantee that leaves maintain normal levels of photosynthesis (Liu, Xiu, Chen, & Jie, 2014). Spraying COS-RA and COS-VA reduced the number of free radicals such as O_2^- and H_2O_2 in the leaves, which improved the leaves' immunity for growth under stress conditions.

Chitosan and chitooligosaccharides can promote plant development and photosynthesis in plant leaves. According to previous study, spraying chitosan on coffee seedlings enhanced photosynthesis, increasing leaf area by 60.53% and total chlorophyll content by 15.36% (Dzung, Khanh, & Dzung, 2011). Compared to COS, COS-VA and COS-RA treatments significantly increased leaf area and leaf thickness (Fig. S3A, B, F), particularly the thickness of fenestrated and spongy tissue (Fig. S3C, D). Moreover, the effectiveness of leaf photosynthesis is also reflected in the amount of leaf area, leaf thickness, fenestration, and spongy tissue. In this study, the principal component analysis indicated that the antioxidant system and photosynthesis were extremely positively correlated. Moreover, after 15 days of COS-RA and COS-VA treatment, SPAD, P_n, and F_v/F_m were considerably greater than those of the control and COS treatment, and mature leaf photosynthetic assimilation products were enhanced. Previously, chitoheptaose treatment of wheat seedlings promoted increased photosynthesis and increased aboveground soluble sugar, soluble protein, and chlorophyll contents by 59.4%, 22.0%, and 20.3%, respectively (Zhang et al., 2016). Therefore, we speculate that COS-VA and COS-RA, due to their strong antioxidant capacity, regulate the antioxidant system and promote leaf structural growth, which in turn increases leaf chlorophyll content and photosynthetic intensity, allowing leaves to accumulate more assimilated products and providing the basis for fruit sugar accumulation.

Sugars and anthocyanins in grape berries increase as a result of the accumulation of leaf assimilation products. It has been demonstrated that chitosan increases photosynthesis, carbon metabolism, and nitrogen metabolism in plants, promoting the buildup of soluble sugars (Ahmed, Khan, Siddiqui, & Jahan, 2020). Chitosan treatment induces the rapid accumulation of various phenolic compounds, including anthocyanins, in grapes (Meng & Tian, 2009). The spraying of COS-VA and COS-RA considerably boosted the soluble solids, total anthocyanin, and soluble sugars content of the berries in this research compared to COS treatment, along with a more than 2-fold increase in sucrose content (Fig. 2D). Several studies have shown that sucrose is involved in the induction of anthocyanin accumulation in plants and that glucose is the main sugar feedstock for anthocyanin synthesis in fruits, including apple (Liu et al., 2017) and grapes (Xia et al., 2021). The current findings revealed that total anthocyanins were significantly and positively correlated with sucrose and glucose content and higher contents of sucrose and glucose promoted the accumulation of anthocyanins, which suggest that COS-VA and COS-RA treatments enhanced the accumulation of sucrose and glucose in grape berries through photosynthesis. This could be one of the causes of the increased anthocyanin production in grapes.

An important indicator of color development in grapes is the anthocyanin level. The primary anthocyanin components found in berries, Mal-3-O-glu, Petu-3-O-ace-glu, and Del-3-O-glu, were also key contributors to the development of grape color (Xia et al., 2021). Compared to COS, the COS-VA and COS-RA treatments resulted in more accumulation of the three monomeric anthocyanins (Fig. 3C–E), which was the main reason why chitosan derivatives contributed to early color development and the high accumulation of total anthocyanins in grapes. Anthocyanin accumulation was accomplished through the control of the expression of genes associated with anthocyanin metabolism, which were highly and positively connected with the total anthocyanin content in grape skin (Fig. 5). Some studies have demonstrated that chitosan or chitooligosaccharides can encourage the synthesis of anthocyanin-like secondary metabolites by inducing high expression of phenylalanine aminolysis (PAL) genes in grape (Meng & Tian, 2009). In this investigation, we discovered that after 15 days, the transcript levels of VvPAL were dramatically elevated by COS-VA and COS-RA treatment, providing one of the strongest indications that chitosan-phenolic acid derivatives induced an increase in grape anthocyanins. VvF3′H, a regulatory gene for dihydroquercetin production, was unaffected, but the high expression of VvF3′5′H at 15 days of treatment stimulated greater dihydroquercetin synthesis (Fig. 5E, F). Dihydroflavonol-4-reductase (DFR) converts dihydromyricetin and dihydroquercetin into the colorless precursors delphinidin and cornflowerin, which are used to make petuniain, mallowin, and Peonidin, respectively (Kühn Weber & Godoy Santin, 2014). As a result, COS-VA and COS-RA treatment encouraged greater Mal-3-O-glu, Petu-3-O-ace-glu, and Del-3-O-glu accumulation (Fig. 4C–E). Moreover, the anthocyanin is inherently unstable and undergoes glycosylation at the C3 position under the action of flavonoid glycosyltransferase (UFGT), which stabilizes it by binding it to glucose. VvMYBA1 and VvMYBA2 are important transcription factors that

directly control UFGT (Kobayashi, Goto-Yamamoto, & Hirochika, 2004). This is supported by the findings of the current study, which showed that COS-VA and COS-RA treatments increased the expression of VvMYBA1 and VvMYBA2, which in turn induced the high expression of VvUFGT in the grape epidermis at 30–45 days.

5. Conclusion

According to the current study, COS was successfully grafted with four phenolic acids, which enhanced antioxidant activity. Spraying grape leaves and fruits with 250 mg L^{-1} solutions of COS-RA and COS-VA during the color-changing period encouraged the accumulation of anthocyanins in the fruit skin. The compounds might have induced this change by enhancing leaf structural development and antioxidant activity, enhancing leaf photosynthesis, increasing the sucrose and glucose content of leaves and fruits, and promoting total anthocyanin accumulation through high sugar levels. Meanwhile, COS-RA and COS-VA promoted the upregulated expression of specific genes related to anthocyanin synthesis (including *PAL*, *F3H*, *F3′5′H*, *DFR*, and *UFGT*), which in turn boosted the accumulation of monomeric anthocyanins (Mal-3-O-glu, Petu-3-O-ace-glu, Del-3-O-glu). Therefore, the application of chitooligosaccharide derivatives could be an effective approach to improve the quality and production of grapes in hot and rainy areas.

Funding

This work was supported by the Science and Technology Planning Project of Guangzhou (No.202206010064, 2023E04J0191) and the National Key Research and Development Program of China (2016YFD0200405-5).

CRediT authorship contribution statement

Songpo Duan: Methodology, Conceptualization, Investigation, Visualization, Formal analysis, Data curation, Writing – original draft, Writing – review & editing. (First author) **Zhiming Li:** Investigation, Visualization, Formal analysis, Data curation, Writing – review & editing. (Co-first author, in second place) **Zaid Khan:** Formal analysis, Data curation. **Chunmei Yang:** Data curation. **Bosi Lu:** Data curation. **Hong Shen:** Conceptualization, Project administration, Funding acquisition.

Declaration of Competing Interest

The authors declare that they have no known competing financial interests or personal relationships that could have appeared to influence the work reported in this paper.

Data availability

No data was used for the research described in the article.

Appendix A. Supplementary data

Supplementary data to this article can be found online at https://doi.org/10.1016/j.fochx.2023.100770.

References

Ahmed, K. B. M., Khan, M. M. A., Siddiqui, H., & Jahan, A. (2020). Chitosan and its oligosaccharides, a promising option for sustainable crop production-a review. *Carbohydrate Polymers, 227*, Article 115331.

Amoah, S. K., Sandjo, L. P., Kratz, J. M., & Biavatti, M. W. (2016). Rosmarinic acid–pharmaceutical and clinical aspects. *Planta Medica, 82*(05), 388–406.

Božič, M., Gorgieva, S., & Kokol, V. (2012). Laccase-mediated functionalization of chitosan by caffeic and gallic acids for modulating antioxidant and antimicrobial properties. *Carbohydrate Polymers, 87*(4), 2388–2398.

Božič, M., Štrancar, J., & Kokol, V. (2013). Laccase-initiated reaction between phenolic acids and chitosan. *Reactive and Functional Polymers, 73*(10), 1377–1383.

Cho, M. J., Howard, L. R., Prior, R. L., & Clark, J. R. (2004). Flavonoid glycosides and antioxidant capacity of various blackberry, blueberry and red grape genotypes determined by high-performance liquid chromatography/mass spectrometry. *Journal of the Science of Food and Agriculture, 84*(13), 1771–1782.

Cui, D., Yang, J., Lu, B., Deng, L., & Shen, H. (2022). Extraction and characterization of chitin from Oratosquilla oratoria shell waste and its application in Brassica campestris L. ssp. *International Journal of Biological Macromolecules, 198*, 204–213.

Deng, Q., Xia, H., Lin, L., Wang, J., Yuan, L., Li, K., … Liang, D. (2019). SUNRED, a natural extract-based biostimulant, application stimulates anthocyanin production in the skins of grapes. *Scientific Reports, 9*(1), 1–8.

Dzung, N. A., Khanh, V. T. P., & Dzung, T. T. (2011). Research on impact of chitosan oligomers on biophysical characteristics, growth, development and drought resistance of coffee. *Carbohydrate Polymers, 84*(2), 751–755.

Fachel, F. N. S., Dal Prá, M., Azambuja, J. H., Endres, M., Bassani, V. L., Koester, L. S., … Braganhol, E. (2020). Glioprotective effect of chitosan-coated rosmarinic acid nanoemulsions against lipopolysaccharide-induced inflammation and oxidative stress in rat astrocyte primary cultures. *Cellular and Molecular Neurobiology, 40*(1), 123–139.

Feng, F., Sun, J., Radhakrishnan, G. V., Lee, T., Bozsóki, Z., Fort, S., … Andersen, K. R. (2019). A combination of chitooligosaccharide and lipochitooligosaccharide recognition promotes arbuscular mycorrhizal associations in Medicago truncatula. *Nature communications, 10*(1), 5047.

Frederickson Matika, D. E., & Loake, G. J. (2014). Redox regulation in plant immune function. *Antioxidants & Redox Signaling, 21*(9), 1373–1388.

Gao, J. (2006). *Experimental guidance for plant physiology*. Beijing, Chinese: China Higher Education Press.

Hu, Q., & Luo, Y. (2016). Polyphenol-chitosan conjugates: Synthesis, characterization, and applications. *Carbohydrate Polymers, 151*, 624–639.

Huerta-Madronal, M., Caro-Leon, J., Espinosa-Cano, E., Aguilar, M. R., & Vázquez-Lasa, B. (2021). Chitosan-Rosmarinic acid conjugates with antioxidant, anti-inflammatory and photoprotective properties. *Carbohydrate Polymers, 273*, Article 118619.

İlyasoğlu, H., & Guo, Z. (2019). Water soluble chitosan-caffeic acid conjugates as a dual functional polymeric surfactant. *Food Bioscience, 29*, 118–125.

Kim, S.-K., & Rajapakse, N. (2005). Enzymatic production and biological activities of chitosan oligosaccharides (COS): A review. *Carbohydrate Polymers, 62*(4), 357–368.

Kobayashi, S., Goto-Yamamoto, N., & Hirochika, H. (2004). Retrotransposon-induced mutations in grape skin color. *Science, 304*(5673), 982.

Kühn Weber, N. A., & Godoy Santin, M. F. (2014). Berry ripening: Recently heard through the grapevine.

Li, Y., Zhang, Q., Ou, L., Ji, D., Liu, T., Lan, R., … Jin, L. (2020). Response to the cold stress signaling of the tea plant (Camellia sinensis) elicited by chitosan oligosaccharide. *Agronomy, 10*(6), 915.

Liu, X.-J., An, X.-H., Liu, X., Hu, D.-G., Wang, X.-F., You, C.-X., & Hao, Y.-J. (2017). MdSnRK1. 1 interacts with MdJAZ18 to regulate sucrose-induced anthocyanin and proanthocyanidin accumulation in apple. *Journal of Experimental Botany, 68*(11), 2977–2990.

Liu, J., Lu, J.-F., Kan, J., Tang, Y.-Q., & Jin, C.-H. (2013). Preparation, characterization and antioxidant activity of phenolic acids grafted carboxymethyl chitosan. *International Journal of Biological Macromolecules, 62*, 85–93.

Liu, J., Yue, R., Si, M., Wu, M., Cong, L., Zhai, R., … Xu, L. (2019). Effects of exogenous application of melatonin on quality and sugar metabolism in 'Zaosu'pear fruit. *Journal of Plant Growth Regulation, 38*, 1161–1169.

Liu, Q.-H., Xiu, W., Chen, B.-C., & Jie, G. (2014). Effects of low light on agronomic and physiological characteristics of rice including grain yield and quality. *Rice Science, 21*(5), 243–251.

Liu, X., Xia, W., Jiang, Q., Yu, P., & Yue, L. (2018). Chitosan oligosaccharide-N-chlorokojic acid mannich base polymer as a potential antibacterial material. *Carbohydrate Polymers, 182*, 225–234.

Malerba, M., & Cerana, R. (2016). Chitosan effects on plant systems. *International Journal of Molecular Sciences, 17*(7), 996.

Meng, X., & Tian, S. (2009). Effects of preharvest application of antagonistic yeast combined with chitosan on decay and quality of harvested table grape fruit. *Journal of the Science of Food and Agriculture, 89*(11), 1838–1842.

Palliotti, A., Tombesi, S., Silvestroni, O., Lanari, V., Gatti, M., & Poni, S. (2014). Changes in vineyard establishment and canopy management urged by earlier climate-related grape ripening: A review. *Scientia Horticulturae, 178*, 43–54.

Saltas, D., Pappas, C. S., Daferera, D., Tarantilis, P. A., & Polissiou, M. G. (2013). Direct determination of rosmarinic acid in Lamiaceae herbs using diffuse reflectance infrared Fourier transform spectroscopy (DRIFTS) and chemometrics. *Journal of Agricultural and Food Chemistry, 61*(13), 3235–3241.

Teixeira, A., Eiras-Dias, J., Castellarin, S. D., & Gerós, H. (2013). Berry phenolics of grapevine under challenging environments. *International Journal of Molecular Sciences, 14*(9), 18711–18739.

Wang, D., Mao, L., Dai, L., Yuan, F., & Gao, Y. (2018). Characterization of chitosan-ferulic acid conjugates and their application in the design of β-carotene bilayer emulsions with propylene glycol alginate. *Food Hydrocolloids, 80*, 281–291.

Whitaker, D. C., Giurcanu, M. C., Young, L. J., Gonzalez, P., Etxeberria, E., Roberts, P., … Roman, F. (2014). Starch content of citrus leaves permits diagnosis of huanglongbing in the warm season but not cool season. *HortScience, 49*(6), 757–762.

Xia, H., Shen, Y., Deng, H., Wang, J., Lin, L., Deng, Q., … Wang, Z. (2021). Melatonin application improves berry coloration, sucrose synthesis, and nutrient absorption in 'Summer Black'grape. *Food Chemistry, 356*, 129–713.

Xia, H., Wang, X., Su, W., Jiang, L., Lin, L., Deng, Q., … Liao, M. (2020). Changes in the carotenoids profile of two yellow-fleshed kiwifruit cultivars during storage. *Postharvest Biology and Technology, 164*, 111–162.

Yu, B., Wang, M., Teng, B., Veeraperumal, S., Cheung, P.-C.-K., Zhong, S., & Cheong, K.-L. (2023). Partially acid-hydrolyzed porphyran improved dextran sulfate sodium-induced acute colitis by modulation of gut microbiota and enhancing the mucosal barrier. *Journal of Agricultural and Food Chemistry, 71*(19), 7299–7311.

Zhang, B., Li, Y., Zhang, Y., Qiao, H., He, J., Yuan, Q., … Fan, J. (2019). High-cell-density culture enhances the antimicrobial and freshness effects of Bacillus subtilis S1702 on table grapes (Vitis vinifera cv. Kyoho). *Food Chemistry, 286*, 541–549.

Zhang, J., Sun, X., Chen, Y., Mi, Y., Tan, W., Miao, Q., … Guo, Z. (2020). Preparation of 2, 6-diurea-chitosan oligosaccharide derivatives for efficient antifungal and antioxidant activities. *Carbohydrate Polymers, 234*, Article 115903.

Zhang, X., Li, K., Liu, S., Xing, R., Yu, H., Chen, X., & Li, P. (2016). Size effects of chitooligomers on the growth and photosynthetic characteristics of wheat seedlings. *Carbohydrate Polymers, 138*, 27–33.

Zhao, D., Wang, J., Tan, L., Sun, C., & Dong, J. (2013). Synthesis of N-furoyl chitosan and chito-oligosaccharides and evaluation of their antioxidant activity in vitro. *International Journal of Biological Macromolecules, 59*, 391–395.

Zou, P., Li, K., Liu, S., Xing, R., Qin, Y., Yu, H., … Li, P. (2015). Effect of chitooligosaccharides with different degrees of acetylation on wheat seedlings under salt stress. *Carbohydrate Polymers, 126*, 62–69.

Zou, P., Tian, X., Dong, B., & Zhang, C. (2017). Size effects of chitooligomers with certain degrees of polymerization on the chilling tolerance of wheat seedlings. *Carbohydrate Polymers, 160*, 194–202.